Scientific Research and Essays Vol. 5(20), pp. 3082-3094, 18 October, 2010
Available online at http://www.academicjournals.org/SRE
ISSN 1992-2248 ©2010 Academic Journals

Full Length Research Paper

Robust decentralized load frequency control in multi-area electric power system using quantitative feedback theory

Shoorangiz Shams, Shamsabad Farahani, Reza Hemati and Mehdi Nikzad*

Department of Electrical Engineering, Islamic Azad University, Islamshahr branch, Iran.

Accepted 17 August, 2010

The load frequency control (LFC) problem has been one of the major subjects in electric power system design and operation. LFC is becoming much more significant today in accordance with increasing size, changing structure and complexity in interconnected power systems. Practice LFC systems use simple proportional-integral (PI) controllers, but parameters of PI controllers are usually tuned based on the trial-and-error approaches and they are incapable to obtain good dynamic performance under a wide range of operating conditions. For this problem, in this paper quantitative feedback theory (QFT) method is used for LFC problem. A multi-area electric power system with a wide range of parametric uncertainties is given to illustrate proposed method. To show effectiveness of proposed method, a classical PI type controller optimized by genetic algorithms (GA) is designed to compare with QFT controller. The simulation results visibly show the validity of QFT method in comparison with traditional method.

Key words: Multi-area electric power system, electric power system load frequency control, robust control, quantitative feedback theory method.

INTRODUCTION

For large scale power systems with interconnected areas, load frequency control (LFC) is important to keep the system frequency and the inter-area tie power as near to the scheduled values as possible. The input mechanical power to the generators is used to control the frequency of output electrical power and to maintain the power exchange between the areas as scheduled. A well designed and operated power system must cope with changes in the load and with system disturbances, and it should provide acceptable high level of power quality while maintaining both voltage and frequency within tolerable limits.

Many control strategies for load frequency control in power systems had been proposed by researchers over the past decades. This extensive research is due to fact that LFC constitutes an important function of power system operation where the main objective is to regulate the output power of each generator at prescribed levels while keeping the frequency fluctuations within pre-specifies limits. robust adaptive control schemes had been developed by Lim et al. (1996), Wang et al. (1998) and Stankovic et al. (1998) to deal with changes in system parametric under LFC strategies. A different algorithm has been presented by Taher and Hematti, (2008) to improve the performance of multi-area power systems. Viewing a multi-area power system under LFC as a decentralized control design for a multi-input multi-output system, it has been shown by Yamashita and Miagi, (1991) that a group of local controllers with tuning parameters can guarantee the overall system stability and performance. The reported results demonstrate clearly the importance of robustness and stability issue in LFC design. In addition, several practical and theoretical issues have been addressed by Xiaofeng and Tomsovic, (2004), Doolla and Bhatti (2006), Grigor'ev (2005) and

*Corresponding author. E-mail: mehdi.nikzad@yahoo.com. Tel: +982188043167, +989122261946. Fax: +982188043167.

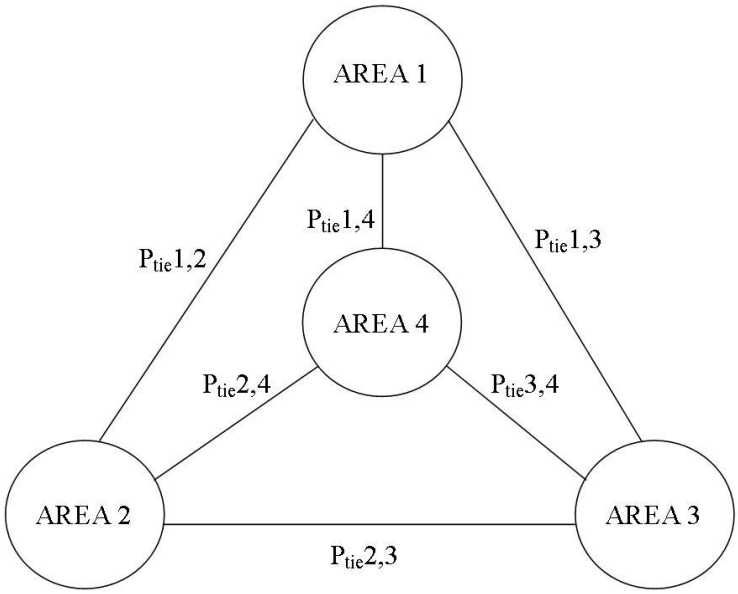

Figure 1. Four-area electric power system with interconnections.

Gvozdev and Samkharadze (2005), which include recent technology utilized by vertically integrated utilities, augmentation of filtered area control error with LFC schemes and hybrid LFC that encompasses an independent system operator and bilateral LFC. The applications of artificial neural network, genetic algorithms and optimal control to LFC have been reported by Hematti et al. (2008), Rerkpreedapong et al. (2003) and Liu et al. (2003).

Many practical systems are characterized by high uncertainty which makes it difficult to maintain good stability margins and performance properties for the closed loop system. There are two general design methodologies for dealing with the effects of uncertainty: (1) Adaptive control, in which the parameters of the plant are identified online and the information obtained is then used to tune the controller, and (2) Robust control, which typically involves a worst-case design approach for family of plants (representing the uncertainty) using a single fixed controller. In this paper, a robust control method (QFT technique) is used for LFC problem. QFT is a robust control method developed during the last two decades which deals with the effects of uncertainty systematically. It has been successfully applied to the design of both SISO (single input - single output) and MIMO (multi input - multi output) systems. It has also been extended to the nonlinear and time-varying cases. QFT often results in simple controllers which are easy to implement (Dazzo and Houpis, 1988; Horowitz, 1979, 1982).

The objective of this paper is to investigate the load frequency control problem for a multi-area electric power system while taking into consideration the uncertainties in the parameters of system. A robust decentralized control scheme is designed using quantitative feedback theory (QFT) method. The proposed method is simulated for a four-area power system. To show effectiveness of proposed method, the proposed controllers are compared to classical PI type controllers optimized by genetic algorithms. Simulation results show that the QFT controllers guarantee robust performance under a wide range of operating conditions and have better performance than the optimized PI type controllers.

PLANT MODEL

A four-area electric power system is considered as a test system and shown in Figure 1.

The block diagram for each area of interconnected areas is shown in Figure 2 (Wood and Wollenberg, 2003):

$B_i = (1/R_i) + D_i$: Frequency bias factor of i^{th} area

ΔP_{tie} ij: Inter area tie power interchange from i^{th} area to j^{th} area.

where, I = 1, 2, 3, 4, j = 1, 2, 3, 4 and I≠j

The inter-area tie power interchange is as (1) (Wood and Wollenberg, 2003):

$$(\Delta Ptieij = (\Delta\omega i - \Delta\omega j) \times (Tij/S) \quad (1)$$

where, $T_{ij} = 377 \times (1/X_{tie}ij)$ (for a 60 Hz system), $X_{tie}ij$: impedance of transmission line between i and j areas.

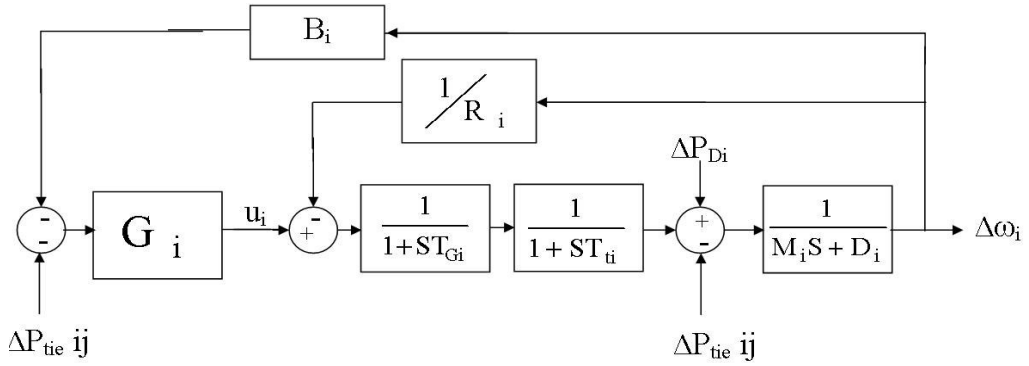

Figure 2. Block diagram for one area of system (i^{th} area). The parameters in Figure 2 are defined as follow: Δ, Deviation from nominal value; $M_i = 2H$, Constant of inertia of i^{th} area; D_i, Damping constant of i^{th} area; R_i, Gain of speed droop feedback loop of i^{th} area; T_{ti}, Turbine Time constant of i^{th} area; T_{Gi}, Governor Time constant of i^{th} area; G_i, Controller of i^{th} area; ΔP_{Di}, Load change of i^{th} area; u_i, Reference load of i^{th} area.

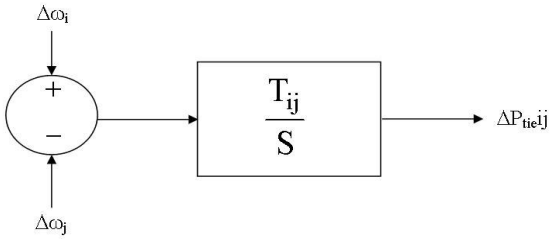

Figure 3. Block diagram of inter area tie power ($\Delta P_{tie}ij$).

The ΔP_{tie} ij block diagram is shown as Figure 3.

Figure 2 shows the block diagram of i^{th} area and Figure 3 shows the method of interconnection between i^{th} and j^{th} areas. The state-space model of four-area interconnected power system is as shown in Equation (2) (Wood and Wollenberg, 2003).

$$\begin{cases} \dot{X} = AX + BU \\ Y = CX \end{cases} \quad (2)$$

Where:

U = [ΔP_{D1} ΔP_{D2} ΔP_{D3} ΔP_{D4} u_1 u_2 u_3 u_4]

Y = [$\Delta\omega_1$ $\Delta\omega_2$ $\Delta\omega_3$ $\Delta\omega_4$ $\Delta P_{tie}1,2$ $\Delta P_{tie}1,3$ $\Delta P_{tie}1,4$ $\Delta P_{tie}2,3$ $\Delta P_{tie}2,4$ $\Delta P_{tie}3,4$

X = [ΔP_{G1} ΔP_{T1} $\Delta\omega_1$ ΔP_{G2} ΔP_{T2} $\Delta\omega_2$ ΔP_{G3} ΔP_{T3} $\Delta\omega_3$ ΔP_{G4} ΔP_{T4} $\Delta\omega_4$ $\Delta P_{tie}1,2$ $\Delta P_{tie}1,3$ $\Delta P_{tie}1,4$ $\Delta P_{tie}2,3$ $\Delta P_{tie}2,4$ $\Delta P_{tie}3,4$]

The matrixes A and B in (2) and the typical values of system parameters for nominal operating condition are given in appendix. The system parametric uncertainties are obtained by 40% changing parameters from their typical values. Based on these uncertainties, some operating conditions are defined and given in appendix.

PROBLEM SPECIFICATION

After system modeling, the controllers are simultaneously designed based on the QFT technique. These controllers have been shown in Figure 2 as G_i. Since four controllers should be simultaneously designed, therefore the problem is a 4 × 4 MIMO problem. To design controller in this system, the design technique for MIMO systems should be considered. SSince controller design for MIMO systems is a sophisticate procedure, so in first, the MIMO system is converted to equivalent MISO (multi input - single output) systems and then controllers are designed for these MISO systems. Using fixed point theory (Horowitz, 1979) the MIMO problem for a m×m system can be decentralized into m equivalent single-loop MISO systems. Each MISO system design is based upon the specifications relating its output and all of its inputs. The basic MIMO compensation structure for a m×m MIMO system is shown in Figure 4; it consists of the uncertain plant matrix P and the diagonal compensation matrix G. These matrices have been shown in Equation (3):

$$P(s) = [P_{ij}](s) = \begin{bmatrix} P_{11} & P_{12} & \cdots & P_{1m} \\ P_{21} & P_{22} & \cdots & P_{2m} \\ \vdots & \vdots & \cdots & \vdots \\ P_{m1} & P_{m2} & \cdots & P_{mm} \end{bmatrix}$$

$$G(s) = \mathrm{diag}\{G_i(s)\} = \begin{bmatrix} G_1 & 0 & 0 & 0 \\ 0 & G_2 & 0 & 0 \\ 0 & 0 & \ddots & 0 \\ 0 & 0 & 0 & G_m \end{bmatrix} \quad (3)$$

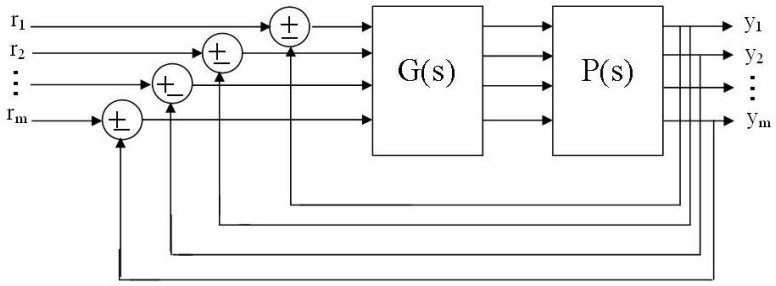

Figure 4. The MIMO control structure for a m×m system.

Fixed point theory develops a mapping that permits the analysis and synthesis of a MIMO control system by a set of equivalent MISO control systems. For m×m system, this mapping results m equivalent systems, each with m inputs and one output. One input is designated as a desired input and the others as disturbance inputs. The inverse of the plant matrix is represented in Equation (4):

$$P(s)^{-1} = \begin{bmatrix} P^*_{11} & P^*_{12} & \cdots & P^*_{1m} \\ P^*_{21} & P^*_{22} & \cdots & P^*_{2m} \\ \vdots & \vdots & \cdots & \vdots \\ P^*_{m1} & P^*_{m2} & \cdots & P^*_{mm} \end{bmatrix} \quad (4)$$

The m effective plant transfer functions are formed as shown in Equation (5):

$$q_{ij} = \frac{1}{P^*_{ij}} = \frac{\det \cdot P}{adj \cdot P_{ij}} \quad (5)$$

There is a requirement that determine P to be minimum phase. The Q matrix is then formed as shown in Equation (6).

$$Q = \begin{bmatrix} q_{11} & q_{12} & \cdots & q_{1m} \\ q_{21} & q_{22} & \cdots & q_{2m} \\ \vdots & \vdots & \ddots & \vdots \\ q_{m1} & q_{m2} & \cdots & q_{mm} \end{bmatrix} = \begin{bmatrix} \frac{1}{P^*_{11}} & \frac{1}{P^*_{12}} & \cdots & \frac{1}{P^*_{1m}} \\ \frac{1}{P^*_{21}} & \frac{1}{P^*_{22}} & \cdots & \frac{1}{P^*_{2m}} \\ \vdots & \vdots & \cdots & \vdots \\ \frac{1}{P^*_{m1}} & \frac{1}{P^*_{m2}} & \cdots & \frac{1}{P^*_{mm}} \end{bmatrix} \quad (6)$$

The matrix P^{-1} is partitioned as (7)

$$P^{-1} = \left[P^*_{ij}\right] = \left[\frac{1}{q_{ij}}\right] = \Lambda + B \quad (7)$$

where Λ is the diagonal part and B is the balance of P^{-1}. The system control ration (system transfer function) relating r to y is given in Equation (8):

$$T = [I+PG]^{-1}PGF \quad (8)$$

Pre-multiplying both sides of Equation (8) by [I+PG] yields Equation (9):

$$[I+PG]\ T = PGF \quad (9)$$

When P is nonsingular, Pre-multiplying both sides of Equation (9) by P^{-1} yields Equation (10):

$$(10)\ [P\text{-}1+G]\ T = GF \quad (10)$$

Using Equation (6) and with G diagonal, Equation (10) can be rearranged as given in Equation (11):

$$T = [\Lambda+G]\text{-}1[GF\text{-}BT] \quad (11)$$

This equation is used to define the desired fixed point mapping where each of the m matrix elements on the right side of (11) can be interpreted as a MISO problem. Proof of the fact that design of each MISO system yields a satisfactory MIMO design is based on the schauder fixed point theorem (Horowitz, 1979).

Based on the above discussions, in this study the LFC control problem specifications are as follow:

1. Number of controllers: 4 controllers for 4 areas
2. Plant matrix P(S) is a 4 × 4 matrix

Diagonal compensation matrix G contains four compensators G_1, G_2, G_3 and G_4

Using dynamic state-space model of the power system presented in (2), the plant transfer function matrix P(S) is obtained with the related inputs and outputs which are shown in Figure 5. Where, the P(S) is uncertain plant transfer function of system and it is clear that the P(S) is a 4×4 matrix. Using Figure 5, the structure of the control system can be shown as Figure 6.

Where the P(S) is obtained using the state space model of the system presented in (2) at any operating condition, G_1, G_2, G3 and G_4 are cascade compensators

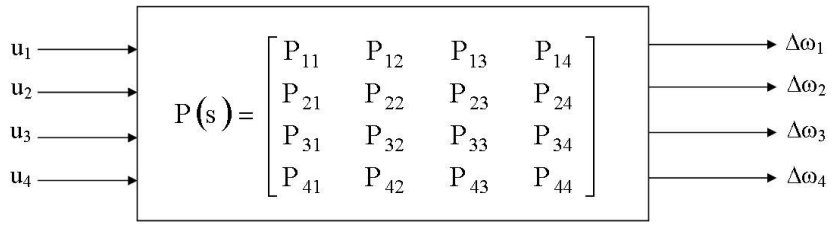

Figure 5. Open-loop system for load frequency control.

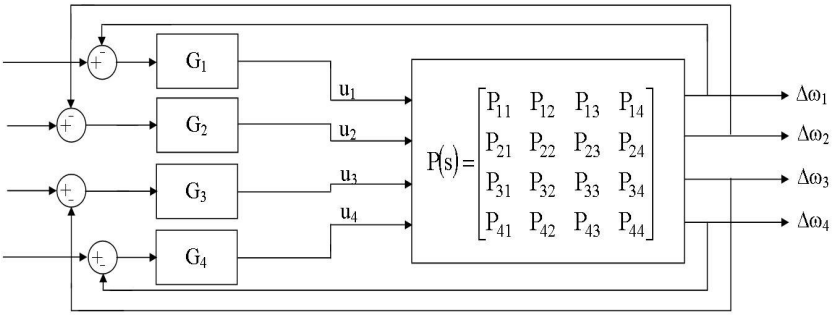

Figure 6. Closed-loop system for load frequency control.

which are designed so that the variations of $\Delta\omega$ and ΔP_{tie} (system outputs) be within the acceptable range under a wide range of operating conditions.

The system operating conditions have been given in appendix. According to these operating conditions and plant transfer function for any operating condition, the effective plant transfer functions defined in (5) (q_{11} , q_{22}, q_{33} and q_{44}) are obtained at any operating condition. Then, according to fixed point theory, first area controller (G_1) is designed based on the effective plant transfer function q_{11} and second area controller (G_2) is designed based on the effective plant transfer function q_{22} and etc. In fact the MIMO problem is converted to four MISO problems. In the next part, the controller design process for these MISO systems is proposed using QFT method.

CONTROLLERS DESIGN USING QFT METHOD

In this investigation, the QFT method is proposed for load frequency control. This approach is briefly developed.

QFT method

Quantitative Feedback Theory (QFT) is a unified theory that emphasizes the use of feedback for achieving the desired system performance tolerances despite plant uncertainty and plant disturbances. QFT quantitatively formulates these two factors as following form:

(1) Sets $\tau_R = \{T_R\}$ of acceptable command or tracking input-output relations and sets $\tau_D = \{T_D\}$ of acceptable disturbance input-output relations.
(2) Sets $\rho = \{P\}$ of possible plants.

The object is to guarantee that the control ratio (system transfer function) $T_R = Y/R$ is a member of τ_R and $T_D = Y/D$ is a member of τ_D for all P(S) in ρ. QFT is essentially a frequency-domain technique and in this paper is used for multiple input – single output (MISO) systems. It is possible to convert the MIMO system into its equivalent sets of MISO systems to which the QFT design technique is applied. The objective is to solve the MISO problems, that is, to find compensation functions which guarantee that the performance tolerance of each MISO problem is satisfied for all P in ρ. The detailed step-by-step procedure to design controllers using QFT technique is given by Dazzo and Houpis, (1988) and Horowitz (1979, 1982).

First area controller design

In this research, the frequency control importance of all four areas is considered as equal. Based on the descriptions above, the structure of control system for i^{th} area is as shown in Figure 7. It is clearly seen that the system is a MISO system and compensator G_1 will be designed based on q_{11}.

Base on QFT technique (Dazzo and Houpis, 1988;

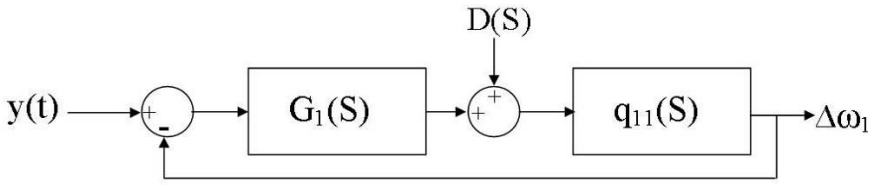

Figure 7. The structure of control system for first area.

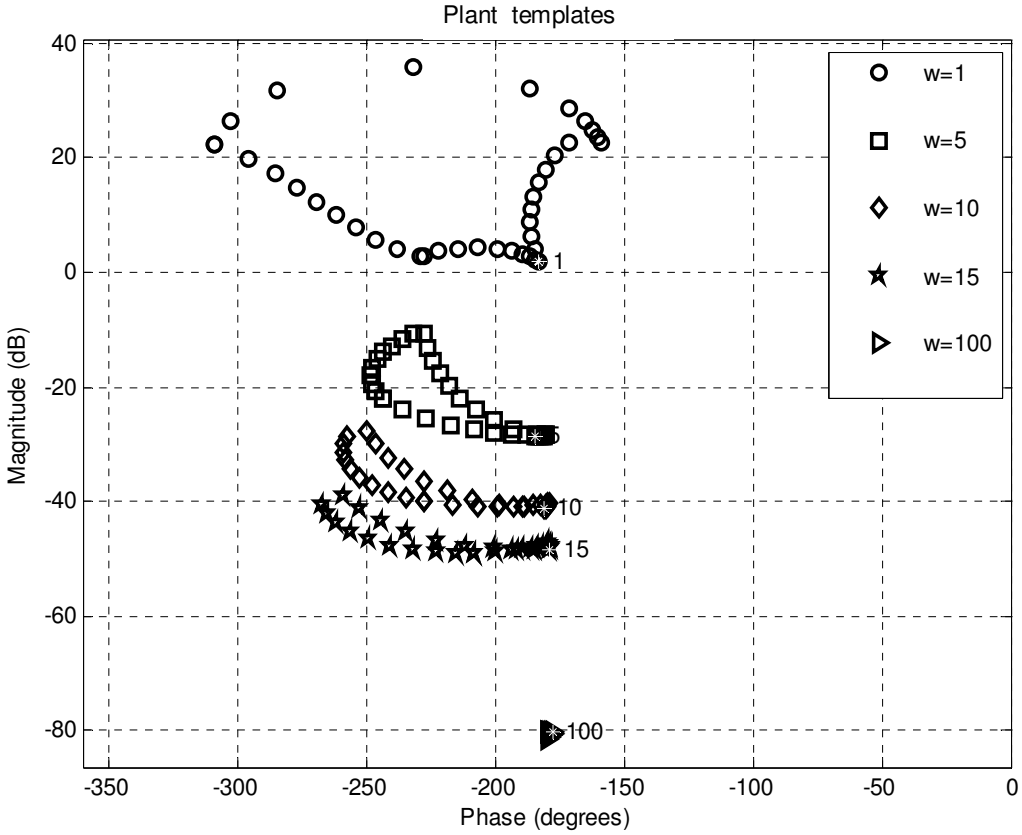

Figure 8. Templates of effective plant transfer function q_{11}.

Horowitz, 1979, 1982) the first step in the design process is to plot the plant uncertainties in Nichols diagram. This plot is known as system templates. The Templates of q_{11} at various operating conditions are obtained by MATLAB software in some frequencies and shown in Figure 8. The compensator G_1 is a cascade compensator and designed so that the variation of output response ($\Delta\omega_1$) be within the acceptable range under the uncertainties of q_{11}. The templates of q_{11} for various operating conditions are shown in Figure 8.

In LFC problem, the output signals such as $\Delta\omega$ or ΔP_{ti} should drive back to zero after step change in demand and in fact the system outputs are regulated by controllers. It means that in LFC problem, the controllers with regulatory characteristics and tracking characteristics are not considered. Therefore considering the tracking specifications is not necessary and consequently the tracking bounds are not considered for LFC problem. But for disturbance rejection purposes, the disturbance rejection bounds are considered to design compensator G1. It should be noted that input disturbance rejection bounds are considered to design controllers. The output response ($\Delta\omega_1$) is acceptable if its magnitude be below the limits given by the disturbance rejection bounds. Based on the desired performance specifications, the disturbance rejection bounds are obtained according to QFT method using QFT toolbox of MATLB software. Since in this case the tracking bounds have not been

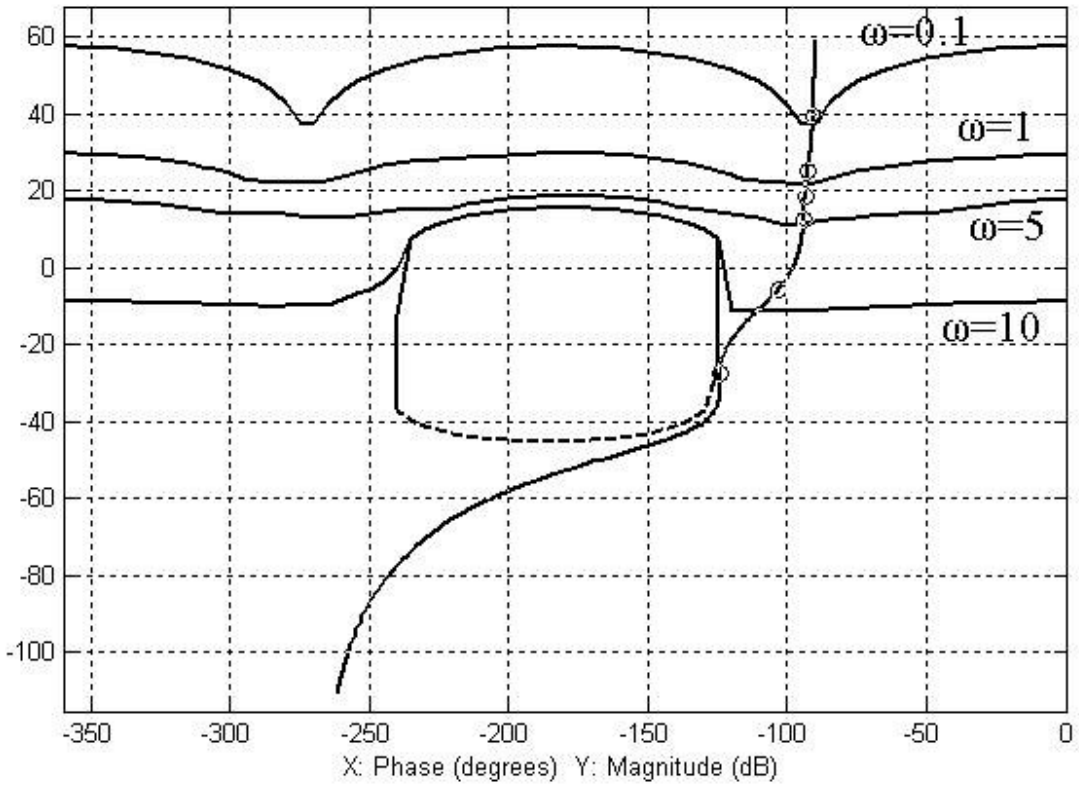

Figure 9. Composite bounds, U-contour and an optimum loop shaping for first area controller design.

considered, so the disturbance rejection bounds (B_D (jωi)) are considered as composite bounds (B_O (jωi)). Also, minimum damping ratios ζ for the dominant roots of the closed-loop system is considered as ζ = 1.2, this amount, on the Nichols chart establishes a region which must not be penetrated by the template of loop shaping (L_O) for all frequencies. The boundary of this region is referred to as U-contour. The U-contour and composite bounds (B_O (jωi)) and an optimum loop shaping (L_1) based these bounds are shown in Figure 9. The transfer function L_1 is as given in Equation (12).

$$L_1 = \frac{14327.51(S+21.92)(S+3.34)}{S(S+5.84)(S+24.7)(S^2+31.54S+2371)} \quad (12)$$

$$G_1(s) = \frac{L_1(s)}{q_{11}(s)} = \frac{186.56\ \ (S+2.34)(S+19.87)}{S\ \ (S^2+134.87S+1895.34)} \quad (13)$$

Using (12) the compensators G_1 is obtained as in (13).

Figure 9 shows that the nominal open-loop transfer function (loop-shaping) is exactly based QFT bounds and according to QFT theory, the design objectives have been met.

The other areas controllers

Since all four areas have the same specifications and features, the controller design for the other areas is like that for the first area and developed method is applied to design the other areas controllers. Using developed method in section 4.2, the compensators G_2, G_3 and G_4 are obtained as follow:

$$G_2(s) = \frac{L_2(s)}{q_{22}(s)} = \frac{636.25\ \ (S+1.34)(S+18.63)}{S\ \ (S^2+142.19S+1632.308)} \quad (14)$$

$$G_3(s) = \frac{L_3(s)}{q_{33}(s)} = \frac{498.22\ \ (S+1.076)(S+9.29)}{S\ \ (S+26.83)(S+93.17)} \quad (15)$$

$$G_4(s) = \frac{L_4(s)}{q_{44}(s)} = \frac{283.68\ \ (S+3.71)(S+18.25)}{S\ \ (S+32.2)(S+111.8)} \quad (16)$$

RESULTS

Here, different comparative cases are considered to show the effectiveness of QFT controllers. These cases

Table 1. Optimum values of KP and KI for PI controllers.

	K_P	K_I
First area controller (G_1	1.8674	5.2070
Second area controller (G_2)	3.1846	4.2829
Third area controller (G_3)	2.4916	2.6287
Fourth area controller (G_4)	1.8912	5.8094

Table 2. Step increase in demand of 1st area (ΔP_{D1}).

Operating condition	Performance index	
	QFT controllers	Optimized PI controllers
1	0.963	1.1373
2	0.9759	1.3261
3	1.0342	1.3285
4	1.0522	1.1974
5	1.3650	1.9430

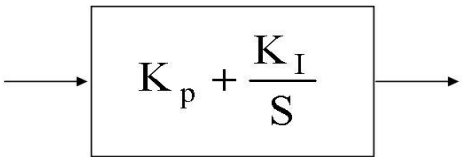

Figure 10. The structure of PI type controller.

have been simulated by MATLAB software. To compare and show effectiveness of QFT method, a classical PI type controller optimized by Genetic Algorithms (GA) is designed for LFC. The structure of PI type controller is shown in Figure 10.

The optimum value of the Parameters K_P and K_I for PI controllers optimized using GA have been obtained and summarized in the Table 1 (Randy and Sue, 2004). In GA case, a continuous type of GA has been used and also performance index for GA optimization has been considered as shown in Equation (17):

$$\text{Performance index} = \int_0^t t|\Delta\omega_1|dt + \int_0^t t|\Delta\omega_2|dt + \int_0^t t|\Delta\omega_3|dt + \int_0^t t|\Delta\omega_4|dt + \int_0^t t|\Delta P_{ti12}|dt + \int_0^t t|\Delta P_{ti13}|dt + \int_0^t t|\Delta P_{ti14}|dt + \int_0^t t|\Delta P_{ti23}|dt + \int_0^t t|\Delta P_{ti24}|dt + \int_0^t t|\Delta P_{ti34}|dt \quad (17)$$

The classical method to compare QFT and optimized PI responses is to show responses following step change at inputs. The responses $\Delta P_{tie}12$, $\Delta P_{tie}13$, $\Delta P_{tie}14$, $\Delta P_{tie}23$, $\Delta P_{tie}24$, $\Delta P_{tie}34$, $\Delta\omega_1$, $\Delta\omega_2$, $\Delta\omega_3$ and $\Delta\omega_4$ should be showed to comparison purposes. Since showing many figures is not favorable, so defined performance index in (17) can be considered for more comparison purposes.

In fact performance index is the total area under the curves (output responses) and this performance index is a suitable benchmark to compare QFT controllers and optimized PI controllers with each other. The parameter "t" in performance index is the simulation time and in simulation, the parameter "t" is considered form zero to settling time of response. It is clear to understand that the controller with lower performance index is better than the other controller or in other words, the controller with lower performance index has better performance than the other controller. The performance index has been calculated following step change at inputs in several operating conditions (The operating conditions have been given in appendix). The results are shown as Tables 2 to 5. It is seen that following step change at different inputs, QFT controllers have better performance than optimized PI controllers at all operating conditions. QFT controllers have lower performance index in comparison with optimized PI controllers and therefore the QFT controllers can damp power system oscillations successfully. Although the Tables result are enough to compare two methods, but it can be useful to show responses in figures. For more comparison purposes, three operating conditions are considered as follow:

1. Nominal operating condition (operating condition 1)
2. Heavy operating condition (operating condition 3)
3. Very heavy operating condition (operating condition 5)

Figure 11 shows $\Delta\omega_1$ at nominal, heavy and very heavy operating conditions following step increase in demand of first area (ΔP_{D1}). It is clear to seen that at all operating conditions QFT controllers have better performance than optimized PI controllers in electric power system control

Table 3. Step increase in demand of 2nd area (ΔP_{D2})

Operating condition	Performance index	
	QFT controllers	Optimized PI controllers
1	1.2190	1.2190
2	1.3214	1.3214
3	1.3512	1.3512
4	1.3730	1.3730
5	2.1759	2.1759

Table 4 . Step increase in demand of 1st area (ΔP_{D1}) and 0.5 step increase in demand of 4th area (ΔP_{D4}.

Operating condition	Performance index	
	QFT controllers	Optimized PI controllers
1	1.0478	1.4313
2	1.0676	1.2166
3	1.1260	1.2620
4	1.1491	1.4324
5	1.4678	2.2888

Table 5. Step increase in demand of 2nd area (ΔP_{D1}) and 0.5 step increase in demand of 3rd area (ΔP_{D3}).

Operating condition	Performance index	
	Optimized PI controllers	QFT controllers
1	1.7159	2.1178
2	1.8169	2.2604
3	1.8301	2.2978
4	1.8480	2.4253
5	3.1800	3.2363

and mitigating oscillations.

DISCUSSION

The simulation results obtained by time domain simulation of electric power system in several different cases are presented. It is obvious that based on these results (tables and figures) the robust controllers have better performance than classical PI type controllers in all operating conditions. The tables and figures clearly show the validity of QFT method for LFC problem and their controllers may be used to increase the flexibility and controllability of power system operation which ends in system stability and cause better utilization of existing power systems.

Due to the fact that the classical controllers are based on nominal operating performances, they cannot guarantee a robust and acceptable performance when either the system parameters or the operating conditions are changeable.

In this paper, robust controllers for a family of plants with changeable system operating condition are presented and it is shown that they are robust under these situations and the system responses are all in acceptable range.

From another point of view, QFT method has better performance and leads to a high order controller in comparison with classic ones but the implementation of these controllers is very complicated and expensive. In general, high order controllers lead to better system performance, whereas the implementation of these controllers need more budgets, while low order controllers lead to poor system performance, but easier implementation. Therefore, choosing a suitable controller depends on the system requirements and importance.

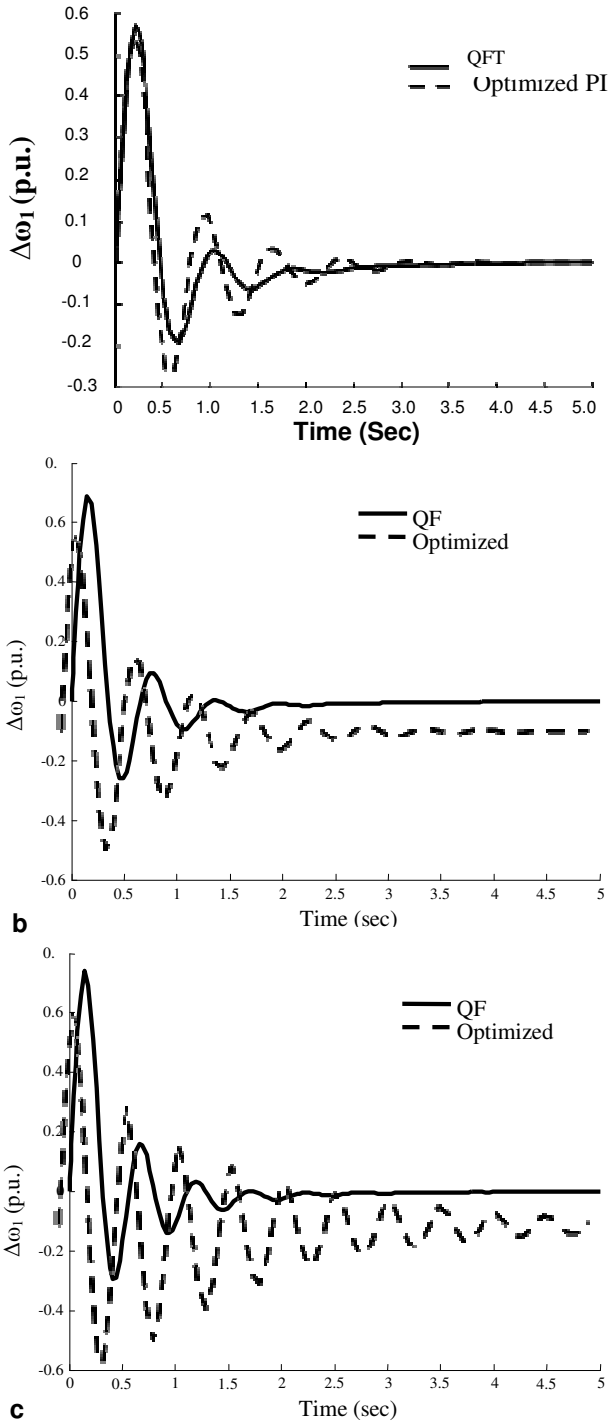

Figure 11. Dynamic response Δω1 following step change in demand of first area (ΔPD1). a: Operating condition 1; b: Operating condition 3; c: Operating condition 5.

Conclusions

In this paper, a new robust approach for Load Frequency Control using QFT method in a four-area electric power system has been successfully proposed. Design strategy includes enough flexibility to setting the desired level of stability and performance, and considering the practical constraint by introducing appropriate uncertainties. The proposed method was applied to a typical four-area power system containing system parametric uncertainties and various loads conditions. Simulation results demonstrated that the designed controllers capable to guarantee the robust stability and robust performance such as precise reference frequency tracking and disturbance attenuation under a wide range of uncertainties and load conditions. Also, the simulation results showed that the QFT method is robust to change in the system parameters and it has better performance than the conventional PI controllers at all operating conditions. As future work, the application of the others robust control methods (such as μ-synthesis and H_∞) can be considered for LFC problem.

REFERENCES

Dazzo JJ, Houpis CH (1988). Linear control system analysis and design: Conventional and modern. McGraw Hill Press. pp. 308-352.
Doolla S, Bhatti TS (2006). Load frequency control of an isolated small-hydro power plant with reduced dump load. IEEE Transactions on Power Systems, 21(4): 1912-1919.
Grigor'ev VI (2005). Methods of load frequency control for generating units of small and micro hydropower plants. Power Technol. Eng., 39(1): 241-254.
Gvozdev BI, Samkharadze RG (2005). Automatic load frequency control of the united power system of siberia. Power Technol. Eng., 39(1): 283-295.
Hematti R, Taher SA, Abdolalipour A (2008). Optimal decentralized load frequency control using HPSO algorithm in deregulated power systems. Am. J. Appl. Sci., 5(9): 1167-1174.
Horowitz IM (1979). Quantitative synthesis of the uncertain multiple input-output feedback systems. Int. J. Control, 30(1): 81-106.
Horowitz IM (1982). Quantitative feedback theory. IEEE Proceedings, 129(6).
Lim KY, Wang Y, Zhou R (1996). Robust decentralized load frequency control of multi-area power system. IEE Proceedings- Generation, Transmission and Distribution, 143(5): 377-386.
Liu F, Song YH, Ma J, Mai S, Lu Q (2003). Optimal load frequency control in restructured power systems. IEE Proceedings-Generation, Transmissions and Distribution, 150(1): 87-95.
Randy LH, Sue EH (2004). Practical genetic algorithms. John Wiley and Sons, pp. 51-65.
Rerkpreedapong D, Hasanovic A, Feliachi A (2003). Robust load frequency control using genetic algorithms and linear mmatrix inequalities. IEEE Transactions on Power Systems, 18(2): 855-861.
Stankovic AM, Tadmor G, Sakharuk TA (1998). Robust control analysis and design for load frequency regulation. IEEE Transactions on Power Systems, 13(2): 449-455.
Taher SA, Hematti R (2008). Robust decentralized load frequency control using multi variable QFT method in deregulated power systems. Am. J. Appl. Sci., 5 (7): 818-828.
Wang Y, Hill DJ, Guo G (1998). Robust decentralized control for multi-machine power system. IEEE Transactions on Circuits and Systems, 45(3):1024-1039.
Wood AJ, Wollenberg BF (2003). Power generation, operation and control. John Wiley and Sons, pp. 328-360.
Xiaofeng YU, Tomsovic K (2004). Application of linear matrix inequalities for load frequency control with communication delays. IEEE Transactions on Power Systems, 19(3): 473-488.

Yamashita K, Miagi H (1991). Multi variable self-tuning regulator for load frequency control system with interaction of voltage on load demand. IEE Proceedings on Control Theory and Applications, 138(2): 177-183.

APPENDIX

The typical values of system parameters for the nominal operating condition are as follow:

1st area parameter			
$T_{T1} = 0.03$	$T_{G1} = 0.08$	$M_1 = 0.1667$	$R_1 = 2.4$
$D_1 = 0.0083$	$B_1 = 0.401$	$T_{12} = 0.425$	$T_{13} = 0.500$
$T_{14} = 0.400$	$T_{23} = 0.455$	$T_{24} = 0.523$	$T_{34} = 0.600$
TT2 = 0.025	TG2 = 0.091	M2=0.1552	R2 = 2.1
2nd area parameter			
D2 = 0.009	B2 = 0.300	T12 = 0.425	T13 = 0.500
T14 = 0.400	T23 = 0.455	T24 = 0.523	T34 = 0.600
TT3 = 0.044	TG3 = 0.072	M3 = 0.178	R3 = 2.9
3rd area parameter			
D3 = 0.0074	B3 = 0.480	T12 =0.425	T13 = 0.500
T14 = 0.400	T23 = 0.455	T24 = 0.523	T34 = 0.600
TT4 = 0.033	TG4 = 0.085	M4 = 0.1500	R4 = 1.995
4th area parameter			
D4 =0.0094	B4 = 0.3908	T12 = 0.425	T13 = 0.500
T14 = 0.400	T23 = 0.455	T24 = 0.523	T34 = 0.600

By ±40% changing parameters from their typical values the system uncertainties are obtained and then system operating conditions can be defined in the uncertainties area. Five operating conditions are defined as follow:

Operating condition 1	
Nominal operating condition	
Operating condition 2	
1st area parameters × -5%	2nd area parameters × +10%
3rd area parameters × -15%	4th area parameters × +12%
Operating condition 3	
1st area parameters × -20%	2nd area parameters × +15%
3rd area parameters × -15%	4th area parameters × +22%
Operating condition 4	
1st area parameters × +25%	2nd area parameters × -25%
3rd area parameters × +30%	4th area parameters × -32%
Operating condition 5	
1st area parameters × +30%	2nd area parameters × -35%
3rd area parameters × +40%	4th area parameters × -40%

Also the matrixes A and B in (2) are as follow:

$$B=\begin{bmatrix}
0 & 0 & \frac{1}{M_1} & 0 & 0 & 0 & 0 & 0 & 0 & 0 & 0 & 0 & 0 & 0 & 0 & 0 & 0 & 0\\
0 & 0 & 0 & 0 & 0 & \frac{1}{M_2} & 0 & 0 & 0 & 0 & 0 & 0 & 0 & 0 & 0 & 0 & 0 & 0\\
0 & 0 & 0 & 0 & 0 & 0 & 0 & 0 & \frac{1}{M_3} & 0 & 0 & 0 & 0 & 0 & 0 & 0 & 0 & 0\\
0 & 0 & 0 & 0 & 0 & 0 & 0 & 0 & 0 & 0 & 0 & \frac{1}{M_4} & 0 & 0 & 0 & 0 & 0 & 0\\
\frac{1}{T_{G1}} & 0 & 0 & 0 & 0 & 0 & 0 & 0 & 0 & 0 & 0 & 0 & 0 & 0 & 0 & 0 & 0 & 0\\
0 & 0 & 0 & \frac{1}{T_{G2}} & 0 & 0 & 0 & 0 & 0 & 0 & 0 & 0 & 0 & 0 & 0 & 0 & 0 & 0\\
0 & 0 & 0 & 0 & 0 & 0 & \frac{1}{T_{G3}} & 0 & 0 & 0 & 0 & 0 & 0 & 0 & 0 & 0 & 0 & 0\\
0 & 0 & 0 & 0 & 0 & 0 & 0 & 0 & 0 & \frac{1}{T_{G4}} & 0 & 0 & 0 & 0 & 0 & 0 & 0 & 0
\end{bmatrix}$$

$$A=\begin{bmatrix}
\frac{-1}{T_{G1}} & 0 & \frac{-1}{R_1T_{G1}} & 0 & 0 & 0 & 0 & 0 & 0 & 0 & 0 & 0 & 0 & 0 & 0 & 0 & 0 & 0\\
\frac{1}{T_{T1}} & \frac{-1}{T_{T1}} & 0 & 0 & 0 & 0 & 0 & 0 & 0 & 0 & 0 & 0 & 0 & 0 & 0 & 0 & 0 & 0\\
0 & \frac{1}{M_1} & \frac{-D_1}{M_1} & 0 & 0 & 0 & 0 & 0 & 0 & 0 & 0 & 0 & \frac{-1}{M_1} & \frac{-1}{M_1} & \frac{-1}{M_1} & 0 & 0 & 0\\
0 & 0 & 0 & \frac{-1}{T_{G2}} & 0 & \frac{-1}{R_2T_{G2}} & 0 & 0 & 0 & 0 & 0 & 0 & 0 & 0 & 0 & 0 & 0 & 0\\
0 & 0 & 0 & \frac{1}{T_{T2}} & \frac{-1}{T_{T2}} & 0 & 0 & 0 & 0 & 0 & 0 & 0 & 0 & 0 & 0 & 0 & 0 & 0\\
0 & 0 & 0 & 0 & \frac{1}{M_2} & \frac{-D_2}{M_2} & 0 & 0 & 0 & 0 & 0 & 0 & \frac{1}{M_2} & 0 & 0 & \frac{-1}{M_2} & \frac{-1}{M_2} & 0\\
0 & 0 & 0 & 0 & 0 & 0 & \frac{-1}{T_{G3}} & 0 & \frac{-1}{R_3T_{G3}} & 0 & 0 & 0 & 0 & 0 & 0 & 0 & 0 & 0\\
0 & 0 & 0 & 0 & 0 & 0 & \frac{1}{T_{T3}} & \frac{-1}{T_{T3}} & 0 & 0 & 0 & 0 & 0 & 0 & 0 & 0 & 0 & 0\\
0 & 0 & 0 & 0 & 0 & 0 & 0 & \frac{1}{M_3} & \frac{-D_3}{M_3} & 0 & 0 & 0 & 0 & \frac{1}{M_3} & 0 & \frac{1}{M_3} & 0 & \frac{-1}{M_3}\\
0 & 0 & 0 & 0 & 0 & 0 & 0 & 0 & 0 & \frac{-1}{T_{G4}} & 0 & \frac{-1}{R_4T_{G4}} & 0 & 0 & 0 & 0 & 0 & 00\\
0 & 0 & 0 & 0 & 0 & 0 & 0 & 0 & 0 & \frac{1}{T_{T4}} & \frac{-1}{T_{T4}} & 0 & 0 & 0 & 0 & 0 & 0 & 0\\
0 & 0 & 0 & 0 & 0 & 0 & 0 & 0 & 0 & 0 & \frac{1}{M_4} & \frac{-D_4}{M_4} & 0 & 0 & \frac{1}{M_4} & 0 & \frac{1}{M_4} & \frac{1}{M_4}\\
0 & 0 & T_{12} & 0 & 0 & -T_{12} & 0 & 0 & 0 & 0 & 0 & 0 & 0 & 0 & 0 & 0 & 0 & 0\\
0 & 0 & T_{13} & 0 & 0 & 0 & 0 & 0 & -T_{13} & 0 & 0 & 0 & 0 & 0 & 0 & 0 & 0 & 0\\
0 & 0 & T_{14} & 0 & 0 & 0 & 0 & 0 & 0 & 0 & 0 & -T_{14} & 0 & 0 & 0 & 0 & 0 & 0\\
0 & 0 & 0 & 0 & 0 & T_{23} & 0 & 0 & -T_{23} & 0 & 0 & 0 & 0 & 0 & 0 & 0 & 0 & 0\\
0 & 0 & 0 & 0 & 0 & T_{24} & 0 & 0 & 0 & 0 & 0 & -T_{24} & 0 & 0 & 0 & 0 & 0 & 0\\
0 & 0 & 0 & 0 & 0 & 0 & 0 & 0 & T_{34} & 0 & 0 & -T_{34} & 0 & 0 & 0 & 0 & 0 & 0
\end{bmatrix}$$